New Lower Bounds for the Number of Pseudoline Arrangements

Adrian Dumitrescu* Ritankar Mandal†

Abstract

Arrangements of lines and pseudolines are fundamental objects in discrete and computational geometry. They also appear in other areas of computer science, such as the study of sorting networks. Let B_n be the number of nonisomorphic arrangements of n pseudolines and let $b_n = \log_2 B_n$. The problem of estimating B_n was posed by Knuth in 1992. Knuth conjectured that $b_n \leq \binom{n}{2} + o(n^2)$ and also derived the first upper and lower bounds: $b_n \leq 0.7924(n^2 + n)$ and $b_n \geq n^2/6 - O(n)$. The upper bound underwent several improvements, $b_n \leq 0.6988n^2$ (Felsner, 1997), and $b_n \leq 0.6571n^2$ (Felsner and Valtr, 2011), for large n. Here we show that $b_n \geq cn^2 - O(n \log n)$ for some constant $c > 0.2053$. In particular, $b_n \geq 0.2053\, n^2$ for large n. This improves the previous best lower bound, $b_n \geq 0.1887n^2$, due to Felsner and Valtr (2011). Our arguments are elementary and geometric in nature. Further, our constructions are likely to spur new developments and improved lower bounds for related problems, such as in topological graph drawings.

Keywords: counting, pseudoline arrangement, recursive construction.

1 Introduction

Arrangements of pseudolines. A *pseudoline* in the Euclidean plane is an x-monotone curve extending from negative infinity to positive infinity. An *arrangement of pseudolines* is a family of pseudolines where each pair of pseudolines has a unique point of intersection (called '*vertex*'). An arrangement is *simple* if no three pseudolines have a common point of intersection, see Fig. 1 (left). Here the term arrangement always means simple arrangement if not specified otherwise.

There are several representations and encodings of pseudoline arrangements. These representations help one count the number of arrangements. Three classic representations are *allowable sequences* (introduced by Goodman and Pollack, see, e.g., [10, 11]), *wiring diagrams* (see for instance [8]), and *zonotopal tilings* (see for instance [7]). A *wiring diagram* is an Euclidean arrangement of pseudolines consisting of piece-wise linear 'wires', each horizontal except for a short segment where it crosses another wire. Each pair of wires cross exactly once. The wiring diagram in Fig. 1 (center) represents the arrangement $\mathcal{A}$. The above representations have been shown to be equivalent; bijective proofs to this effect can be found in [7]. Wiring diagrams are also known as *reflection networks*, i.e., networks that bring n wires labeled from 1 to n into their reflection by means of performing switches of adjacent wires; see [14, p. 35]. Lastly, they are also known under the name of *primitive sorting networks*; see [15, Ch. 5.3.4]. The number of such networks with n wires, i.e., the number of pseudoline arrangements with n pseudolines, is denoted by A_n. Stanley [20] established the following closed formula for A_n:

$$A_n = \frac{\binom{n}{2}!}{\prod_{k=1}^{n-1}(2n-2k-1)^k}$$

Two arrangements are *isomorphic* if they can be mapped onto each other by a homeomorphism of the plane; see Fig. 1. This means that for A_n, the left to right order of the vertices in the arrangement plays a role while for B_n only the order of vertices along each particular pseudoline is important, i.e., the relative position of two vertices from distinct pairs of pseudolines does not matter.

The number of *nonisomorphic* arrangements of n pseudolines is denoted by B_n; this is the number of equivalence classes of all arrangements of n pseudolines; see [14, p. 35]. We are interested in the growth rate of B_n; so let[1] $b_n = \log_2 B_n$. Knuth [14] conjectured that $b_n \leq \binom{n}{2} + o(n^2)$; see also [8, p. 147] and [6, p. 259]. This conjecture is still open.

Upper bounds on the number of pseudoline arrangements. Felsner [6] used a horizontal encoding of an arrangement in order to estimate B_n. An arrangement can be represented by a sequence of horizontal cuts. The ith cut is the list of pseudolines crossing the ith pseudoline in the order of the crossings. Using this approach, Felsner [6, Thm. 1] obtained the upper bound $b_n \leq 0.7213(n^2 - n)$; he then refined this bound by using *replace matrices*. A replace matrix is a binary $n \times n$ matrix M with the properties $\sum_{j=1}^{n} m_{ij} = n - i$ for all i and $m_{ij} \geq m_{ji}$ for all $i < j$. Using this technique, the

*Department of Computer Science, University of Wisconsin–Milwaukee, USA. Email: dumitres@uwm.edu.

†Department of Computer Science, University of Wisconsin–Milwaukee, USA. Email: rmandal@uwm.edu.

[1] Throughout this paper, $\log x$ is the logarithm in base 2 of x.

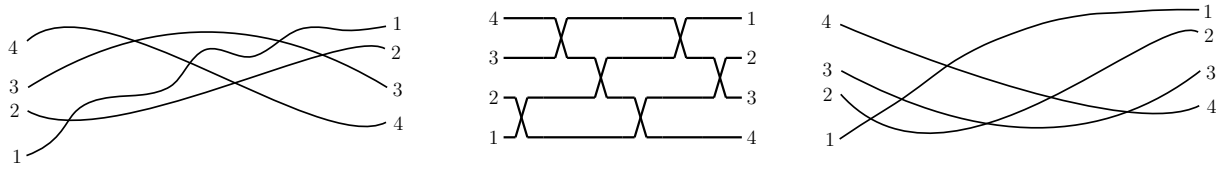

Figure 1: Left: A simple arrangement $\mathcal{A}$. Center: Wiring diagram of $\mathcal{A}$. Right: An arrangement $\mathcal{A}'$ that is not isomorphic to the arrangement $\mathcal{A}$ on the left.

author established the upper bound $b_n < 0.6974\,n^2$ [6, Thm. 2].

In his seminal paper on the topic, Knuth [14] took a vertical approach for encoding. Let $\mathcal{A}$ be an arrangement of n pseudolines $\{\ell_1, \ldots, \ell_n\}$. By adding pseudoline ℓ_{n+1} to $\mathcal{A}$, we get $\mathcal{A}'$, an arrangement of $n+1$ pseudolines. The course of ℓ_{n+1} describes a vertical cutpath from top to bottom. The number of cutpaths of $\mathcal{A}$ is exactly the number of arrangements $\mathcal{A}'$ such that $\mathcal{A}' \setminus \{\ell_{n+1}\}$ is isomorphic to $\mathcal{A}$. Let γ_n denote the maximum number of cutpaths in an arrangement of n pseudolines. Therefore, one has $B_{n+1} \le \gamma_n \cdot B_n$; and $B_3 = 2$. Knuth [14] proved that $\gamma_n \le 3^n$, concluding that $B_n \le 3^{\binom{n+1}{2}}$ and thus $b_n \le 0.5\,(n^2+n)\log_2 3 \le 0.7924\,(n^2+n)$; this computation can be streamlined so that it yields $b_n \le 0.7924\,n^2$, see [9]. Knuth also conjectured that $\gamma_n \le n \cdot 2^n$, but this was refuted by Ondřej Bílka in 2010 [9]; see also [8, p. 147]. Felsner and Valtr [9] proved a refined result, $\gamma_n \le 4n \cdot 2.48698^n$, by a careful analysis. This yields $b_n \le 0.6571\,n^2$, which is the current best upper bound.

Lower bounds on the number of pseudoline arrangements. Knuth [14, p. 37] gave a recursive construction in the setting of reflection networks. The number of nonisomorphic arrangements in his construction, thus also B_n, obeys the recurrence

$$B_n \ge 2^{n^2/8 - n/4} B_{n/2}.$$

By induction this yields $B_n \ge 2^{n^2/6 - 5n/2}$.

Matoušek sketched a simple—still recursive—grid construction in his book [18, Sec. 6.2], see Fig 2. Let n be a multiple of 3 and $m = \frac{n}{3}$ (assume that m is odd). The $2m$ lines in the two extreme bundles form a regular grid of m^2 points. The lines in the central bundle are incident to $\frac{3m^2+1}{4}$ of these grid points. At each such point, there are 2 choices; going below it or above it, thus creating at least $\frac{3m^2}{4} = \frac{3(n/3)^2}{4} = \frac{n^2}{12}$ binary choices. Thus B_n obeys the recurrence

$$B_n \ge 2^{n^2/12} B_{n/3}^3,$$

which by induction yields $B_n \ge 2^{n^2/8}$.

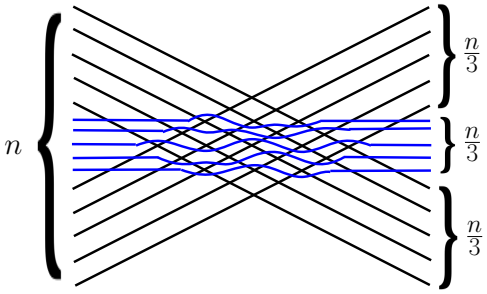

Figure 2: Grid construction for a lower bound on B_n.

Felsner and Valtr [9] used rhombic tilings of a centrally symmetric hexagon in an elegant recursive construction for a lower bound on B_n. Consider a set of $i+j+k$ pseudolines partitioned into the following three parts: $\{1, \ldots, i\}$, $\{i+1, \ldots, i+j\}$, $\{i+j+1, \ldots, i+j+k\}$, see Fig. 3. A partial arrangement is called *consistent* if any two pseudolines from two different parts always cross but any two pseudolines from the same part never cross.

The zonotopal duals of consistent partial arrangements are rhombic tilings of the centrally symmetric hexagon $H(i,j,k)$ with side lengths i, j, k. The enumeration of rhombic tilings of $H(i,j,k)$ was solved by MacMahon [17] (see also [5]), who showed that the number of tilings is

$$P(i,j,k) = \prod_{a=0}^{i-1} \prod_{b=0}^{j-1} \prod_{c=0}^{k-1} \frac{a+b+c+2}{a+b+c+1}. \tag{1.1}$$

A nontrivial (and quite involved) derivation using integral calculus shows that

$$\begin{aligned} \ln P(n,n,n) &= \left(\frac{9}{2}\ln 3 - 6\ln 2\right) n^2 + O(n \log n) \\ &= 1.1323\ldots n^2 + O(n \log n). \end{aligned}$$

Assuming n to be a multiple of 3 in the recursion step, the construction yields the lower bound recurrence

$$B_n \ge P\left(\frac{n}{3}, \frac{n}{3}, \frac{n}{3}\right) B_{n/3}^3. \tag{1.2}$$

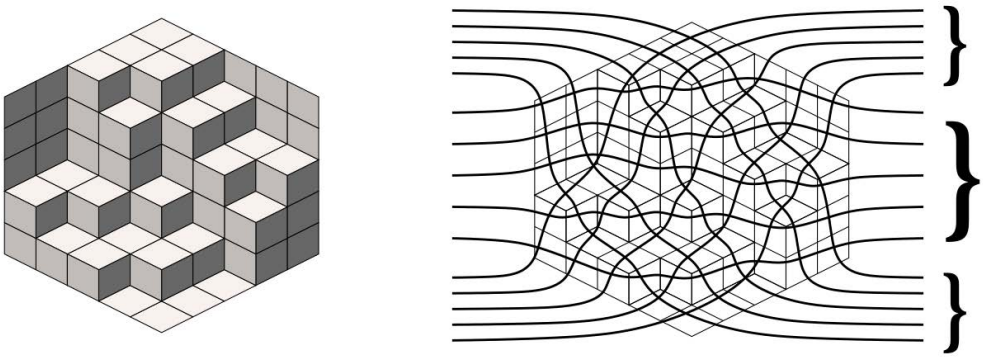

Figure 3: The hexagon $H(5,5,5)$ with one of its rhombic tilings and a consistent partial arrangement corresponding to the tiling. This figure is reproduced from [9].

By induction, the analytic solution to formula (1.1) together with the recurrence (1.2) yield the lower bound $B_n \geq 2^{cn^2 - O(n \log^2 n)}$, where $c = \frac{3}{4}\ln 3 - \ln 2 = 0.1887\ldots$ In particular, $b_n \geq 0.1887n^2$ for large n; this is the previous best lower bound.

Table 1 shows the exact values of A_n and B_n, and their growth rate (up to four digits after the decimal point) with respect to n, for small values of n. The values of B_n for $n = 1$ to 9 are from [14, p. 35] and the values of B_{10}, B_{11}, and B_{12} are from [6], [21], and [19], respectively; the values of B_{13}, B_{14}, and B_{15} have been added recently, see [13, 19]. Observe that A_n grows much faster than B_n.

Our results. Here we extend the method used by Matoušek in his grid construction; observe that it uses lines of 3 slopes. In Sections 2 and 3, we use lines of 8 and 12 different slopes in orthogonal type constructions, yielding the lower bounds $b_n \geq 0.1999n^2$ and $b_n \geq 0.2053n^2$ for large n, respectively. In Section 4, we use lines of 6 different slopes in hexagonal type constructions, yielding the lower bound $b_n \geq 0.1981n^2$ for large n. While the construction in Section 3 gives a better bound, the ones in Sections 2 and 4 are easier to analyze. For each of the two styles, rectangular and hexagonal, the constructions are presented in increasing order of complexity. As such, most (the 2nd part) of Section 2 and the entire Section 4 can be skipped, if so desired. Our main result is summarized in the following.

THEOREM 1.1. *Let B_n be the number of arrangements of n pseudolines. Then $B_n \geq 2^{cn^2 - O(n \log n)}$, for some constant $c > 0.2053$. In particular, $B_n \geq 2^{0.2053n^2}$ for large n.*

Outline of the proof. We construct a line arrangement using lines of k different slopes (for a small k). The final construction will be obtained by a small clockwise rotation, so that there are no vertical lines. Let $m = \lfloor n/k \rfloor$ or $m = \lfloor n/k \rfloor - 1$ (whichever is odd). Each bundle consists of m equidistant lines in the corresponding parallel strip; remaining lines are discarded, or not used in the counting. An *i-wise crossing* is an intersection point of exactly i lines. Let $\lambda_i(m)$ denote the number of i-wise crossings in the arrangement where each bundle consists of m lines. Our goal is to estimate $\lambda_i(m)$ for each i. Then we can locally replace the lines around each i-wise crossing with any of the B_i nonisomorphic pseudoline arrangements; and further apply recursively this construction to each of the k bundles of parallel lines exiting this junction. This yields a simple pseudoline arrangement for each possible replacement choice. Consequently, the number of nonisomorphic pseudoline arrangements in this construction, say, $T(n)$, satisfies the recurrence:

$$T(n) \geq F(n) \left[T\left(\frac{n}{k}\right) \right]^k, \tag{1.3}$$

where $F(n)$ is a multiplicative factor counting the number of choices in this junction:

$$F(n) \geq \prod_{i=3}^{k} B_i^{\lambda_i(n)}. \tag{1.4}$$

Related work. In a comprehensive recent paper, Kynčl [16] obtained estimates on the number of isomorphism classes of simple topological graphs that realize various graphs. The author remarks that it is probably hard to obtain tight estimates on this quantity, "given that even for pseudoline arrangements, the best known lower and upper bounds on their number differ significantly". While our improvements aren't spectacular, it seems however likely that some of the techniques we used here can be employed to obtain sharper lower bounds for topological graph drawings too.

n	A_n	$\frac{\log_2 A_n}{n^2}$	B_n	$\frac{\log_2 B_n}{n^2}$
1	1	0	1	0
2	1	0	1	0
3	2	0.1111	2	0.1111
4	16	0.25	8	0.1875
5	768	0.3833	62	0.2381
6	292,864	0.5044	908	0.2729
7	1,100,742,656	0.6129	24,698	0.2977
8	48,608,795,688,960	0.7104	1,232,944	0.3161
9	29,258,366,996,258,488,320	0.7983	112,018,190	0.3301
10			18,410,581,880	0.3409
11			5,449,192,389,984	0.3496
12			2,894,710,651,370,536	0.3566
13			2,752,596,959,306,389,652	0.3624
14			4,675,651,520,558,571,537,540	0.3672
15			14,163,808,995,580,022,218,786,390	0.3713

Table 1: Values of A_n and B_n for small n.

Notations and formulas used. For two similar figures F, F', let $\rho(F, F')$ denote their similarity ratio. For a planar region R, let area(R) denote its area. By slightly abusing notation, let area(i, j, k) denote the area of the triangle bounded by three lines ℓ_i, ℓ_j and ℓ_k. Assume that the equations of the three lines are $\alpha_s x + \beta_s y + \gamma_s = 0$, for $s = 1, 2, 3$, respectively. Then

$$\text{area}(i,j,k) = \frac{A^2}{2|C_1C_2C_3|}, \text{ where}$$
$$A = \begin{vmatrix} \alpha_1 & \beta_1 & \gamma_1 \\ \alpha_2 & \beta_2 & \gamma_2 \\ \alpha_3 & \beta_3 & \gamma_3 \end{vmatrix},$$
$$C_1 = (\alpha_2\beta_3 - \beta_2\alpha_3),$$
$$C_2 = -(\alpha_1\beta_3 - \beta_1\alpha_3),$$
$$C_3 = (\alpha_1\beta_2 - \beta_1\alpha_2).$$

Let $P(i, j, g, h)$ denote the parallelogram bounded by the pairs of parallel lines $\ell_i \parallel \ell_j$ and $\ell_g \parallel \ell_h$.

2 Preliminary rectangular constructions

Warm-up: a rectangular construction with 4 slopes. We start with a simple rectangular construction with 4 bundles of parallel lines whose slopes are $0, \infty, \pm 1$; see Fig. 4. Let $U = [0, 1]^2$ be the unit square we work with. The axes of all parallel strips are incident to the center of U.

For $i = 3, 4$, let a_i denote the area of the region covered by exactly i of the 4 strips. It is easy to see that $a_3 = a_4 = 1/2$, and obviously $a_3 + a_4 = \text{area}(U) = 1$. Observe that $\lambda_i(m)$ is proportional to a_i, for $i = 3, 4$; taking the boundary effect into account, we have

$$\lambda_3(m) = \frac{m^2}{2} - O(m) \text{ and } \lambda_4(m) = \frac{m^2}{2} - O(m).$$

Since $m = n/4$, λ_i can be also viewed as a function of n. Therefore $\lambda_3(n) = \lambda_4(n) = n^2/32 - O(n)$, and so the multiplicative factor in Eq. (1.3) is bounded from below as follows:

$$F(n) \geq \prod_{i=3}^{4} B_i^{\lambda_i(n)} \geq 2^{n^2/32 - O(n)} \cdot 8^{n^2/32 - O(n)}$$
$$= 2^{n^2/8 - O(n)}.$$

By induction on n, the resulting lower bound is $T(n) \geq 2^{n^2/6 - O(n \log n)}$; this matches the constant $1/6$ in Knuth's lower bound described in Section 1.

Rectangular construction with 8 slopes. We next describe and analyze a rectangular construction with lines of 8 slopes[2]. See Fig. 5. Consider 8 bundles of parallel lines whose slopes are $0, \infty, \pm 1/2, \pm 1, \pm 2$. The axes of all parallel strips are incident to the center of U. This construction yields the lower bound $b_n \geq 0.1999\, n^2$ for large n.

Let $\mathcal{L} = \mathcal{L}_1 \cup \ldots \cup \mathcal{L}_8$ be the partition of $\mathcal{L}$ into eight bundles. The m lines in $\mathcal{L}_i$ are contained in the parallel strip Γ_i bounded by the two lines ℓ_{2i-1} and ℓ_{2i}, for $i = 1, \ldots, 8$. The equation of line ℓ_i is

[2] If desired, the reader can skip to Section 3.

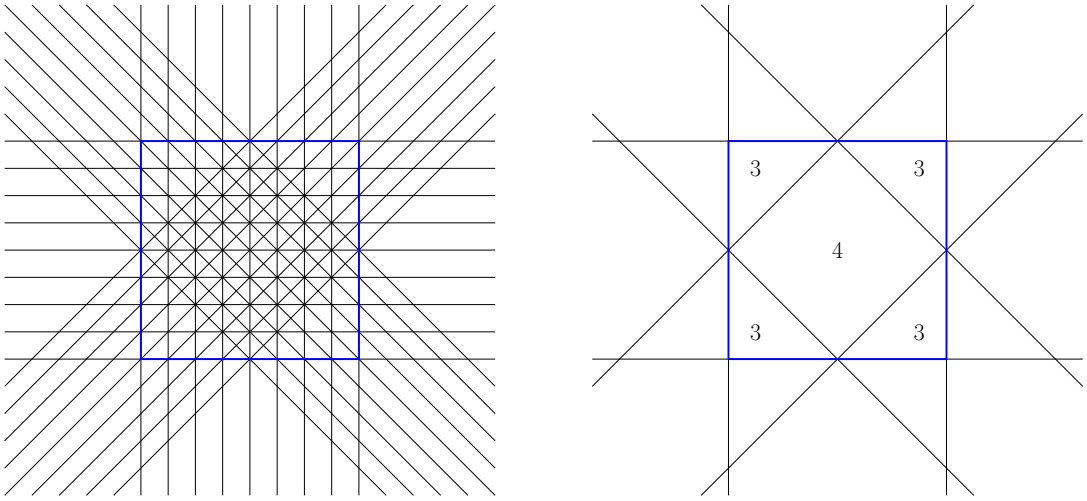

Figure 4: Construction with 4 slopes; here $m = 9$. The unit square $U = [0,1]^2$ is drawn in blue.

$\alpha_i x + \beta_i y + \gamma_i = 0$, with $\alpha_i, \beta_i, \gamma_i$, $i = 1, \ldots, 16$ given in Fig 6 (right). Observe that $U = \Gamma_4 \cap \Gamma_8$.

We refer to lines in $\mathcal{L}_4 \cup \mathcal{L}_8$ (i.e., axis-aligned lines) as the *primary* lines, and to rest of the lines as *secondary* lines. We refer to the intersection points of the primary lines as *grid vertices*. The slopes of the primary lines are in $\{0, \infty\}$. The slopes of the secondary lines are in $\{\pm 1/2, \pm 1, \pm 2\}$.

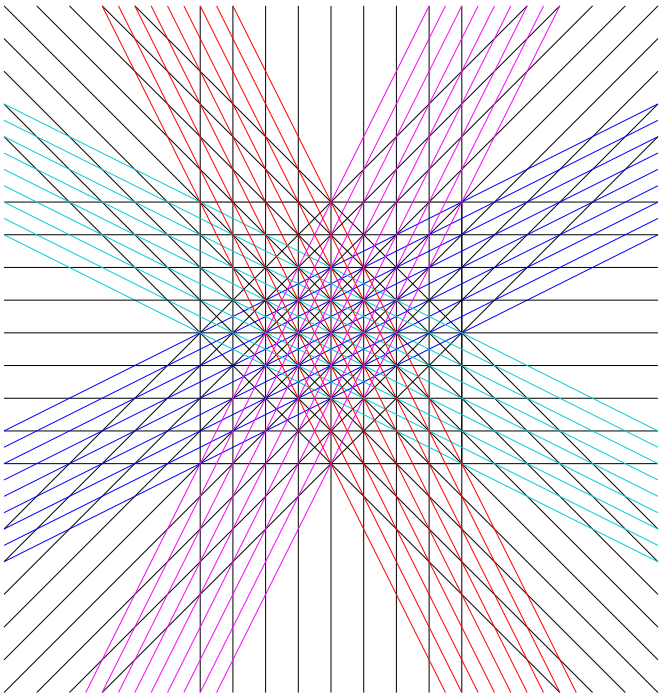

Figure 5: Construction with 8 slopes; here $m = 9$.

- the distance between consecutive lines in $\mathcal{L}_4$ or $\mathcal{L}_8$ is $\frac{1}{m}\left(1 - O\left(\frac{1}{m}\right)\right)$;
- the distance between consecutive lines in $\mathcal{L}_2$ or $\mathcal{L}_6$ is $\frac{1}{m\sqrt{2}}\left(1 - O\left(\frac{1}{m}\right)\right)$;
- the distance between consecutive lines in $\mathcal{L}_1$, $\mathcal{L}_3$, $\mathcal{L}_5$ or $\mathcal{L}_7$ is $\frac{1}{m\sqrt{5}}\left(1 - O\left(\frac{1}{m}\right)\right)$.

Let $\sigma_0 = \sigma_0(m)$ denote the *basic parallelogram* (here, square) determined by consecutive axis-aligned lines (i.e., lines in $\mathcal{L}_4 \cup \mathcal{L}_8$); the side length of σ_0 is $\frac{1}{m}\left(1 - O\left(\frac{1}{m}\right)\right)$. We refer to these basic parallelograms as *grid cells*. Let U' be the smaller square bounded by $\ell_5, \ell_6, \ell_{13}, \ell_{14}$, i.e., $U' = \Gamma_3 \cap \Gamma_7$; the similarity ratio $\rho(U', U)$ is equal to $\frac{1}{\sqrt{5}}$. We have

$$\begin{aligned}
&\text{area}(U) = 1,\\
&\text{area}(U') = \frac{\text{area}(U)}{5} = \frac{1}{5},\\
&\text{area}(\sigma_0) = \frac{1}{m^2}\left(1 - O\left(\frac{1}{m}\right)\right).
\end{aligned}$$

For $i = 3, \ldots, 8$, let a_i denote the area of the (not necessarily connected) region covered by exactly i of the 8 strips. Recall that $\text{area}(i, j, k)$ denotes the area of the triangle bounded by ℓ_i, ℓ_j, and ℓ_k. We have

$$\begin{aligned}
a_3 &= 8 \cdot \text{area}(3, 7, 15) = 1,\\
a_4 &= 8 \cdot \text{area}(5, 7, 11) = \frac{1}{3},\\
a_5 &= 4\left(2 \cdot \text{area}(5, 11, 13) + \text{area}(2, 5, 11)\right) = \frac{7}{30},\\
a_6 &= 4\left(\text{area}(6, 11, 13) - 2 \cdot \text{area}(2, 9, 11)\right.\\
&\quad \left. -\text{area}(2, 9, 13)\right) = \frac{1}{5},\\
a_7 &= 8 \cdot \text{area}(5, 9, 13) = \frac{1}{15},
\end{aligned}$$

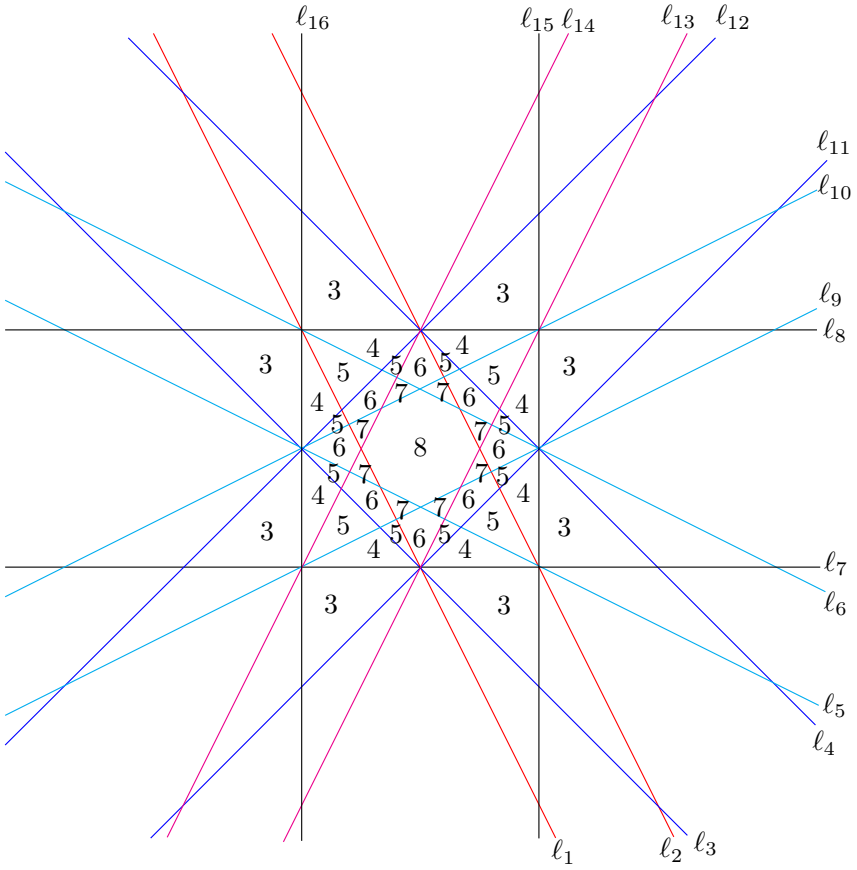

i	α_i	β_i	γ_i
1	2	1	-1
2	2	1	-2
3	1	1	-0.5
4	1	1	-1.5
5	1	2	-1
6	1	2	-2
7	0	1	0
8	0	1	-1
9	1	-2	0
10	1	-2	1
11	1	-1	-0.5
12	1	-1	0.5
13	2	-1	-1
14	2	-1	0
15	1	0	-1
16	1	0	0

Figure 6: Left: The eight parallel strips and the corresponding covering multiplicities. These numbers only reflect incidences at the grid vertices made by the axis-aligned lines. Right: Coefficients of the lines ℓ_i for $i = 1, \ldots, 16$.

$$a_8 = \text{area}(U') - 4 \cdot \text{area}(5, 9, 13) = \frac{1}{5} - \frac{1}{30} = \frac{1}{6}.$$

Observe that $a_4 + a_5 + a_6 + a_7 + a_8 = \text{area}(U) = 1$. Recall that $\lambda_i(m)$ denote the number i-wise crossings where each bundle consists of m lines. Note that $\lambda_i(m)$ is proportional to a_i, for $i = 4, 5, 6, 7, 8$. Indeed, $\lambda_i(m)$ is equal to the number of grid points that lie in a region covered by i parallel strips, which is roughly equal to the ratio $\frac{a_i}{\text{area}(\sigma_0)}$, for $i = 4, 5, 6, 7, 8$. More precisely, taking also the boundary effect of the relevant regions into account, we obtain

$$\lambda_4(m) = \frac{a_4}{\text{area}(\sigma_0)} - O(m) = \frac{m^2}{3} - O(m),$$
$$\lambda_5(m) = \frac{a_5}{\text{area}(\sigma_0)} - O(m) = \frac{7m^2}{30} - O(m),$$
$$\lambda_6(m) = \frac{a_6}{\text{area}(\sigma_0)} - O(m) = \frac{m^2}{5} - O(m),$$
$$\lambda_7(m) = \frac{a_7}{\text{area}(\sigma_0)} - O(m) = \frac{m^2}{15} - O(m),$$
$$\lambda_8(m) = \frac{a_8}{\text{area}(\sigma_0)} - O(m) = \frac{m^2}{6} - O(m).$$

For estimating $\lambda_3(m)$, in addition to considering 3-wise crossings in the exterior of U, we also have 3-wise crossings on the boundaries or in the interior of the small grid squares contained in some regions of U. Specifically, we distinguish exactly four types of 3-wise crossings, as illustrated in Fig. 7 and specified in Table 2. For $j = 1, 2, 3, 4$, let w_j denote the weighted area containing all crossings of type j, where the weight is the number of 3-wise crossings per grid cell. To complete the estimate of $\lambda_3(m)$, we calculate w_j for all j, from the bundles intersecting at crossings of type j; listed in Table 2.

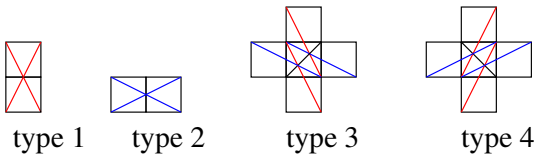

Figure 7: Types of incidences of 3 lines that are not at grid vertices.

Recall that for two parallel strips Γ_i and Γ_j, the

j	Bundles intersecting at vertices of type j
1	$\mathcal{L}_4, \mathcal{L}_1, \mathcal{L}_7$
2	$\mathcal{L}_8, \mathcal{L}_3, \mathcal{L}_5$
3	$\mathcal{L}_6, \mathcal{L}_1, \mathcal{L}_3$
4	$\mathcal{L}_2, \mathcal{L}_5, \mathcal{L}_7$

Table 2: Intersecting bundles for these crossings.

area of their intersection is

$$\text{area}(\Gamma_i \cap \Gamma_j) = \text{area}(P(2i-1, 2i, 2j-1, 2j)),$$

where $P(2i-1, 2i, 2j-1, 2j)$ denotes the parallelogram bounded by the two pairs of parallel lines ℓ_{2i-1}, ℓ_{2i} and ℓ_{2j-1}, ℓ_{2j}, respectively. For types 1 and 2, there is one crossing per grid cell and for types 3 and 4, there are two crossings per grid cell. Therefore we have,

$$\begin{aligned}
w_1 &= \text{area}(\Gamma_4 \cap \Gamma_1 \cap \Gamma_7) = \text{area}(\Gamma_1 \cap \Gamma_7) \\
&= \text{area}(P(1, 2, 13, 14)) = 1/4, \\
w_2 &= \text{area}(\Gamma_8 \cap \Gamma_3 \cap \Gamma_5) = \text{area}(\Gamma_3 \cap \Gamma_5) \\
&= \text{area}(P(5, 6, 9, 10)) = 1/4, \\
w_3 &= 2 \cdot \text{area}(\Gamma_1 \cap \Gamma_3 \cap \Gamma_6) \\
&= 2 \cdot (\text{area}(P(1, 2, 5, 6)) - 2 \cdot \text{area}(2, 5, 11)) \\
&= 2 \cdot (1/3 - 1/12) = 1/2, \\
w_4 &= 2 \cdot \text{area}(\Gamma_2 \cap \Gamma_5 \cap \Gamma_7) = 1/2.
\end{aligned}$$

It follows that

$$\begin{aligned}
\lambda_3(m) &= \frac{a_3 + \sum_{j=1}^{4} w_j}{\text{area}(\sigma_0)} - O(m) \\
&= \left(1 + \frac{1}{4} + \frac{1}{4} + \frac{1}{2} + \frac{1}{2}\right) m^2 - O(m) \\
&= \frac{5m^2}{2} - O(m).
\end{aligned}$$

The values of $\lambda_i(m)$, for $i = 3, 4, 5, 6, 7, 8$, are summarized in Table 3; for convenience the linear terms are omitted. Since $m = n/8$, λ_i can be also viewed as a function of n.

i	3	4	5	6	7	8
$\lambda_i(m)$	$\frac{5m^2}{2}$	$\frac{m^2}{3}$	$\frac{7m^2}{30}$	$\frac{m^2}{5}$	$\frac{m^2}{15}$	$\frac{m^2}{6}$
$\lambda_i(n)$	$\frac{5n^2}{2 \cdot 64}$	$\frac{n^2}{3 \cdot 64}$	$\frac{7n^2}{30 \cdot 64}$	$\frac{n^2}{5 \cdot 64}$	$\frac{n^2}{15 \cdot 64}$	$\frac{n^2}{6 \cdot 64}$

Table 3: The asymptotic values of $\lambda_i(m)$ and $\lambda_i(n)$ for $i = 3, 4, 5, 6, 7, 8$.

The multiplicative factor in Eq. (1.3) is bounded from below as follows:

$$\begin{aligned}
F(n) \geq \prod_{i=3}^{8} B_i^{\lambda_i(n)} &\geq 2^{\frac{5n^2}{2 \cdot 64}} \cdot 8^{\frac{n^2}{3 \cdot 64}} \cdot 62^{\frac{7n^2}{30 \cdot 64}} \cdot 908^{\frac{n^2}{5 \cdot 64}} \\
&\cdot 24698^{\frac{n^2}{15 \cdot 64}} \cdot 1232944^{\frac{n^2}{6 \cdot 64}} \cdot 2^{-O(n)}.
\end{aligned}$$

We prove by induction on n that $T(n) \geq 2^{cn^2 - O(n \log n)}$ for a suitable constant $c > 0$. It suffices to choose c (using the values of B_i for $i = 3, \ldots, 8$ in Table 1) so that

$$\begin{aligned}
\frac{1}{64} \Bigg(&\frac{5}{2} + \frac{1}{3} \log 8 + \frac{7}{30} \log 62 + \frac{1}{5} \log 908 \\
&+ \frac{1}{15} \log 24698 + \frac{1}{6} \log 1232944 \Bigg) \geq \frac{7c}{8}.
\end{aligned}$$

The above inequality holds if we set

$$\begin{aligned}
c = \frac{1}{56} \Bigg(&\frac{5}{2} + 1 + \frac{7}{30} \log 62 + \frac{1}{5} \log 908 \\
&+ \frac{1}{15} \log 24698 + \frac{1}{6} \log 1232944 \Bigg) > 0.1999,
\end{aligned} \tag{2.5}$$

and this yields the lower bound $B_n \geq 2^{cn^2 - O(n \log n)}$, for some constant $c > 0.1999$. In particular, we have $B_n \geq 2^{0.1999n^2}$ for large n.

3 Rectangular construction with 12 slopes

We next describe and analyze a rectangular construction with lines of 12 slopes, which provides our main result in Theorem 1.1. Consider 12 bundles of parallel lines whose slopes are $0, \infty, \pm 1/3, \pm 1/2, \pm 1, \pm 2, \pm 3$. The axes of all parallel strips are incident to the center of $U = [0, 1]^2$. Refer to Fig. 8. This construction yields the lower bound $b_n \geq 0.2053\, n^2$ for large n.

Let $\mathcal{L} = \mathcal{L}_1 \cup \ldots \cup \mathcal{L}_{12}$ be the partition of $\mathcal{L}$ into twelve bundles. The m lines in $\mathcal{L}_i$ are contained in the parallel strip Γ_i bounded by the two lines ℓ_{2i-1} and ℓ_{2i}, for $i = 1, \ldots, 12$. The equation of line ℓ_i is $\alpha_i x + \beta_i y + \gamma_i = 0$, with $\alpha_i, \beta_i, \gamma_i$, $i = 1, \ldots, 24$ given in Table 4. Observe that $U = \Gamma_6 \cap \Gamma_{12}$.

We refer to lines in $\mathcal{L}_6 \cup \mathcal{L}_{12}$ (i.e., axis-aligned lines) as the *primary* lines, and to rest of the lines as the *secondary* lines. We refer to the intersection points of the primary lines as *grid vertices*. The slopes of the primary lines are in $\{0, \infty\}$, and the slopes of the secondary lines are in $\{\pm 1/3, \pm 1/2, \pm 1, \pm 2, \pm 3\}$. Note that

- the distance between consecutive lines in $\mathcal{L}_6$ or in $\mathcal{L}_{12}$ is $\frac{1}{m}\left(1 - O\left(\frac{1}{m}\right)\right)$;
- the distance between consecutive lines in $\mathcal{L}_3$ or in $\mathcal{L}_9$ is $\frac{1}{m\sqrt{2}}\left(1 - O\left(\frac{1}{m}\right)\right)$;

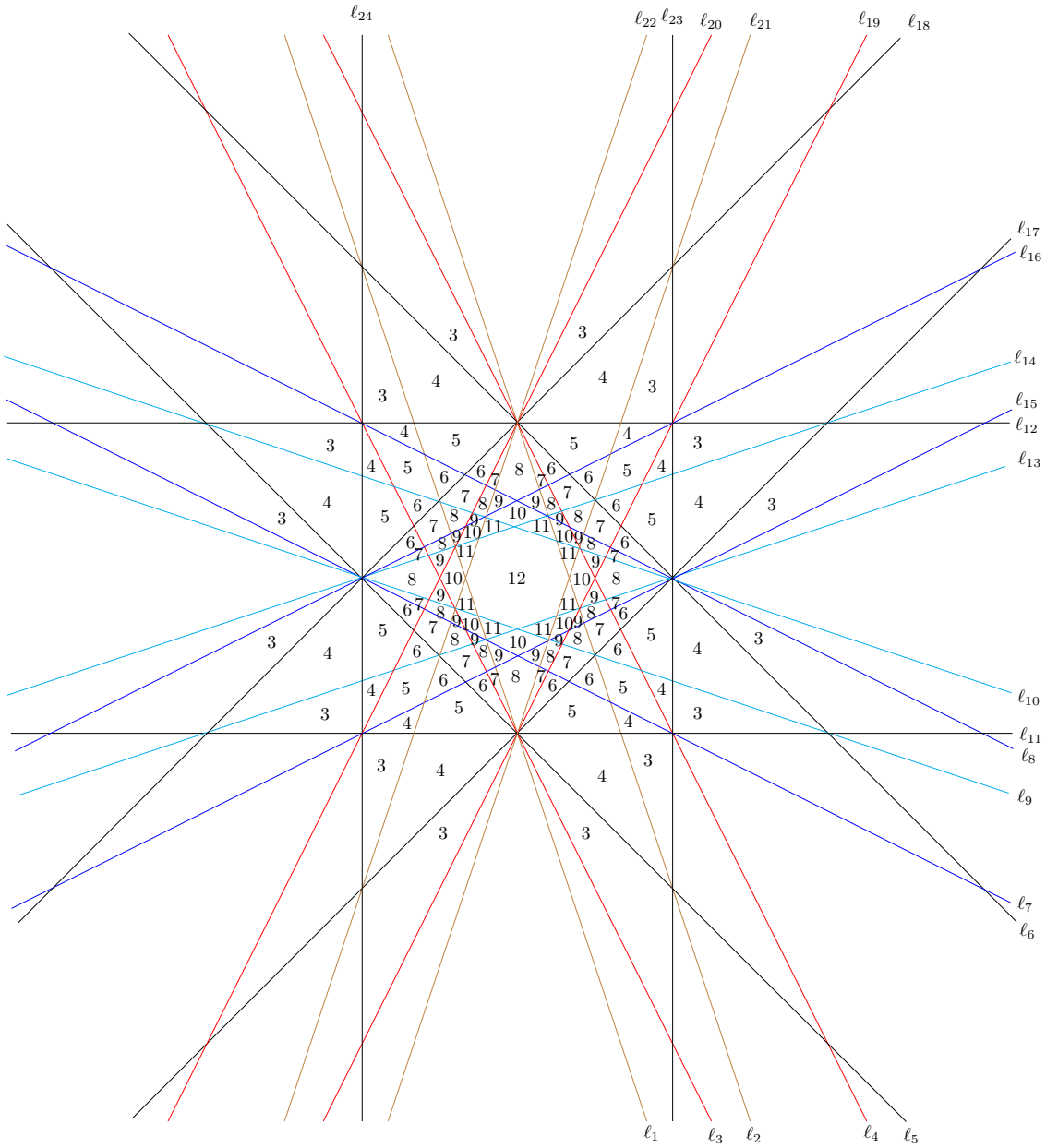

Figure 8: Construction with 12 slopes. The twelve parallel strips and the corresponding covering multiplicities. These numbers only reflect incidences at the grid vertices made by the axis-aligned lines.

i	α_i	β_i	γ_i
1	3	1	-1.5
2	3	1	-2.5
3	2	1	-1
4	2	1	-2
5	1	1	-0.5
6	1	1	-1.5
7	1	2	-1
8	1	2	-2

i	α_i	β_i	γ_i
9	1	3	-1.5
10	1	3	-2.5
11	0	1	0
12	0	1	-1
13	-1	3	-0.5
14	-1	3	-1.5
15	-1	2	0
16	-1	2	-1

i	α_i	β_i	γ_i
17	-1	1	0.5
18	-1	1	-0.5
19	-2	1	1
20	-2	1	0
21	-3	1	1.5
22	-3	1	0.5
23	-1	0	1
24	-1	0	0

Table 4: Coefficients of the 24 lines.

- the distance between consecutive lines in $\mathcal{L}_2$, $\mathcal{L}_4$, $\mathcal{L}_8$, or $\mathcal{L}_{10}$ is $\frac{1}{m\sqrt{5}}\left(1-O\left(\frac{1}{m}\right)\right)$;
- the distance between consecutive lines in $\mathcal{L}_1$, $\mathcal{L}_5$, $\mathcal{L}_7$, or $\mathcal{L}_{11}$ is $\frac{1}{m\sqrt{10}}\left(1-O\left(\frac{1}{m}\right)\right)$.

Let $\sigma_0 = \sigma_0(m)$ denote the basic parallelogram (here, square) determined by consecutive axis-aligned lines (i.e., lines in $\mathcal{L}_6 \cup \mathcal{L}_{12}$); the side length of σ_0 is $\frac{1}{m}\left(1-O\left(\frac{1}{m}\right)\right)$. We refer to these basic parallelograms as *grid cell*. Let U_1 be the smaller square bounded by $\ell_1, \ell_2, \ell_{13}, \ell_{14}$ and let U_2 be the smaller square bounded by $\ell_3, \ell_4, \ell_{15}, \ell_{16}$. Note that $\rho(U_1, U) = \frac{1}{\sqrt{10}}$ and $\rho(U_2, U) = \frac{1}{\sqrt{5}}$. We also have

$$\begin{aligned}
&\text{area}(U) = 1,\\
&\text{area}(U_1) = \frac{\text{area}(U)}{10} = \frac{1}{10},\\
&\text{area}(U_2) = \frac{\text{area}(U)}{5} = \frac{1}{5},\\
&\text{area}(\sigma_0) = \frac{1}{m^2}\left(1-O\left(\frac{1}{m}\right)\right).
\end{aligned}$$

For $i = 3, \ldots, 12$, let a_i denote the area of the (not necessarily connected) region covered by exactly i of the 12 strips. Recall that $\text{area}(i,j,k)$ denotes the area of the triangle bounded by ℓ_i, ℓ_j, and ℓ_k. We have

$$\begin{aligned}
a_3 &= 8\cdot(\text{area}(2,11,13) + \text{area}(3,5,23))\\
&= 8\cdot\left(\frac{1}{8}+\frac{1}{24}\right) = \frac{4}{3},\\
a_4 &= 8\cdot(\text{area}(2,5,11) + \text{area}(2,7,11))\\
&= 8\cdot\left(\frac{1}{12}+\frac{1}{120}\right) = \frac{11}{15},\\
a_5 &= 4\cdot(\text{area}(11,17,23) - 2\cdot\text{area}(2,7,11)\\
&\quad -2\cdot\text{area}(2,7,17)) = 4\left(\frac{1}{8}-\frac{2}{120}-\frac{2}{120}\right) = \frac{11}{30},\\
a_6 &= 4\cdot(2\cdot\text{area}(7,17,19) + 2\cdot\text{area}(2,7,17))\\
&= 4\cdot\left(\frac{2}{120}+\frac{2}{120}\right) = \frac{2}{15},\\
a_7 &= 4\cdot(2\cdot\text{area}(7,19,21) + 2\cdot(\text{area}(9,17,19)\\
&\quad -\text{area}(7,17,19)))\\
&= 4\cdot\left(\frac{1}{140}+2\cdot\left(\frac{1}{56}-\frac{1}{120}\right)\right) = \frac{11}{105},\\
a_8 &= 8\cdot(\text{area}(9,19,21) - \text{area}(7,19,21))\\
&\quad + 4\cdot(\text{area}(2,9,15) - \text{area}(9,15,19))\\
&\quad + 8\cdot\text{area}(7,21,25) = \frac{13}{105},\\
a_9 &= 8\cdot(\text{area}(7,15,21) + \text{area}(9,15,19))\\
&= 8\cdot\left(\frac{1}{280}+\frac{1}{840}\right) = \frac{4}{105},\\
a_{10} &= 4\cdot((\text{area}(7,13,15) - \text{area}(9,13,15))\\
&\quad +(\text{area}(13,19,21) - \text{area}(15,19,21)))\\
&= 4\cdot\left(\left(\frac{1}{40}-\frac{1}{60}\right)+\left(\frac{1}{80}-\frac{1}{120}\right)\right)\\
&= 4\cdot\left(\frac{1}{120}+\frac{1}{240}\right) = \frac{1}{20},\\
a_{11} &= 8\cdot\text{area}(2,13,21) = \frac{8}{240} = \frac{1}{30},\\
a_{12} &= \text{area}(U_1) - 4\cdot\text{area}(9,13,21) = \frac{1}{10}-\frac{4}{240} = \frac{1}{12}.
\end{aligned}$$

Observe that the region whose area is $\sum_{i=4}^{12} a_i$ consists of U and 8 triangles outside U. Therefore,

$$\begin{aligned}
\sum_{i=4}^{12} a_i &= \text{area}(U) + 8\cdot\text{area}(2,5,11)\\
&= 1+\frac{2}{3} = \frac{5}{3}.
\end{aligned}$$

Recall that $\lambda_i(m)$ denote the number i-wise crossings where each bundle consists of m lines. Note that $\lambda_i(m)$ is proportional to a_i, for $i = 7, 8, \ldots, 12$. Indeed, $\lambda_i(m)$ is equal to the number of grid vertices, i.e., intersection points of the axis-parallel lines (i.e., lines in $\mathcal{L}_6 \cup \mathcal{L}_{12}$) that lie in a region covered by i parallel strips, which is roughly equal to the ratio $\frac{a_i}{\text{area}(\sigma_0)}$, for $i = 7, 8, \ldots, 12$. More precisely, taking also the boundary effect of the relevant regions into account, we obtain

$$\begin{aligned}
\lambda_7(m) &= \frac{a_7}{\text{area}(\sigma_0)} - O(m) = \frac{11m^2}{105} - O(m),\\
\lambda_8(m) &= \frac{a_8}{\text{area}(\sigma_0)} - O(m) = \frac{13m^2}{105} - O(m),\\
\lambda_9(m) &= \frac{a_9}{\text{area}(\sigma_0)} - O(m) = \frac{4m^2}{105} - O(m),\\
\lambda_{10}(m) &= \frac{a_{10}}{\text{area}(\sigma_0)} - O(m) = \frac{m^2}{20} - O(m),\\
\lambda_{11}(m) &= \frac{a_{11}}{\text{area}(\sigma_0)} - O(m) = \frac{m^2}{30} - O(m),\\
\lambda_{12}(m) &= \frac{a_{12}}{\text{area}(\sigma_0)} - O(m) = \frac{m^2}{12} - O(m).
\end{aligned}$$

For $i = 3, 4, 5, 6$, not all the i-wise crossings are at grid vertices. It can be exhaustively verified (by hand) that there are 29 types of crossings; see Fig. 9. The bundles intersecting at each of these 29 types of vertices are listed in Table 5. For $j = 1, 2, \ldots, 29$, let w_j denote the weighted area containing all crossings of type j, where the weight is the number of crossings per grid cell.

To complete the estimates of $\lambda_i(m)$ for $i = 3, 4, 5, 6$, we calculate w_j for all j from the bundles intersecting at type j crossings. The values are listed in Table 6.

For $\lambda_6(m)$, all the 6-wise crossings that are not at grid vertices, are at the centers of the grid cells; we have

$$\begin{aligned} w_{29} &= \text{area}(\Gamma_1 \cap \Gamma_3 \cap \Gamma_5 \cap \Gamma_7 \cap \Gamma_9 \cap \Gamma_{11}) \\ &= \text{area}(\Gamma_1 \cap \Gamma_5 \cap \Gamma_7 \cap \Gamma_{11}) = a_{12}. \end{aligned}$$

It follows that

$$\begin{aligned} \lambda_6(m) &= \frac{a_6 + w_{29}}{\text{area}(\sigma_0)} - O(m) = \frac{a_6 + a_{12}}{\text{area}(\sigma_0)} - O(m) \\ &= \frac{2m^2}{15} + \frac{m^2}{12} - O(m) = \frac{13m^2}{60} - O(m). \end{aligned}$$

Similarly for $\lambda_5(m)$, all the 5-wise crossings that are not at grid vertices, i.e., types 25 through 28, are in the interiors of grid cells contained in eight small triangles inside U. For example,

$$\begin{aligned} w_{28} &= \text{area}(\Gamma_1 \cap \Gamma_3 \cap \Gamma_5 \cap \Gamma_7 \cap \Gamma_9 \cap \overline{\Gamma_{11}}) \\ &= \text{area}(1, 14, 22) + \text{area}(2, 13, 21) = \frac{1}{120}. \end{aligned}$$

Observe that sum of the areas of these eight small triangles equals to a_{11}. It follows that

$$\begin{aligned} \lambda_5(m) &= \frac{a_5 + \sum_{j=25}^{28} w_j}{\text{area}(\sigma_0)} - O(m) = \frac{a_5 + a_{11}}{\text{area}(\sigma_0)} - O(m) \\ &= \frac{11m^2}{30} + \frac{m^2}{30} - O(m) = \frac{2m^2}{5} - O(m). \end{aligned}$$

To estimate $\lambda_4(m)$, note that besides 4-wise crossings at grid vertices, there are six types of 4-wise crossings i.e., types 19 through 24, in the interiors of grid cells:

- For types 19 and 20, there is one crossing per grid cell; and

  $$\begin{aligned} w_{19} &= \text{area}(\Gamma_3 \cap \Gamma_5 \cap \Gamma_7 \cap \Gamma_9 \cap \overline{\Gamma_1} \cap \overline{\Gamma_{11}}) \\ &= (\text{area}(2, 10, 13) - \text{area}(2, 10, 21)) \\ &\quad + (\text{area}(9, 14, 22) - \text{area}(1, 14, 22)) = \frac{1}{15}, \end{aligned}$$

  Type 20 is a 90° rotation of type 19; therefore by symmetry, $w_{19} = w_{20}$.

- For types 21 and 22, there is one crossing per grid cell; and

  $$\begin{aligned} w_{21} &= \text{area}(\Gamma_3 \cap \Gamma_7 \cap \Gamma_9 \cap \Gamma_{11} \cap \overline{\Gamma_1} \cap \overline{\Gamma_5}) \\ &= (\text{area}(2, 14, 21) - \text{area}(2, 10, 21)) \\ &\quad + (\text{area}(1, 13, 22) - \text{area}(1, 9, 22)) = \frac{1}{40}. \end{aligned}$$

  Type 22 is the reflection in a vertical line of type 21; therefore by symmetry, $w_{21} = w_{22}$.

- For types 23 and 24, there are four crossings per grid cell; and

  $$\begin{aligned} w_{23} &= 4 \cdot \text{area}(\Gamma_1 \cap \Gamma_4 \cap \Gamma_7 \cap \Gamma_{10}) \\ &= 4 \cdot \text{area}(\Gamma_1 \cap \Gamma_7) = 4 \cdot \text{area}(U_1) = \frac{2}{5}. \end{aligned}$$

  Type 24 is the reflection in a vertical line of type 23; therefore by symmetry, $w_{23} = w_{24}$.

Consequently, we have

$$\begin{aligned} \lambda_4(m) &= \frac{a_4 + \sum_{j=19}^{24} w_j}{\text{area}(\sigma_0)} - O(m) \\ &= \Big(\frac{11}{15} + \frac{2}{15} + \frac{1}{20} + \frac{4}{5}\Big)m^2 - O(m) \\ &= \frac{103m^2}{60} - O(m). \end{aligned}$$

Lastly, we estimate $\lambda_3(m)$. Besides 3-wise crossings at grid vertices, there are 18 types of 3-wise crossings i.e., types 1 through 18, in the interior of grid cells:

- For types 1 and 2, there is one crossing per grid cell; and

  $$\begin{aligned} w_1 &= \text{area}(\Gamma_2 \cap \Gamma_6 \cap \Gamma_{10}) \\ &= \text{area}(\Gamma_2 \cap \Gamma_{10}) = \text{area}(P(3, 4, 19, 20)) = \frac{1}{4}. \end{aligned}$$

  Type 2 is a 90° rotation of type 1; therefore by symmetry, $w_1 = w_2$.

- For types 3 and 4, there are two crossings per grid cell; and

  $$\begin{aligned} w_3 &= 2 \cdot (\text{area}(\Gamma_2 \cap \Gamma_4 \cap \Gamma_9)) \\ &= 2 \cdot (\text{area}(P(3, 4, 7, 8)) \\ &\quad - \text{area}(3, 8, 18) - \text{area}(4, 7, 17)) = \frac{1}{2}. \end{aligned}$$

  Type 4 is the reflection in a vertical line of type 3; therefore by symmetry, $w_3 = w_4$.

- For types $5, 6, 7, 8$, there is one crossing per grid cell; and

  $$\begin{aligned} w_5 &= \text{area}(\Gamma_3 \cap \Gamma_7 \cap \Gamma_9 \cap \overline{\Gamma_1} \cap \overline{\Gamma_5} \cap \overline{\Gamma_{11}}) \\ &= \text{area}(5, 9, 22) + \text{area}(6, 10, 21)) = \frac{1}{20}. \end{aligned}$$

  Type 6 is the reflection in a vertical line of type 5, and types 7 and 8 are 90° rotations of types 6 and 5, respectively. Therefore by symmetry, $w_5 = w_6 = w_7 = w_8$.

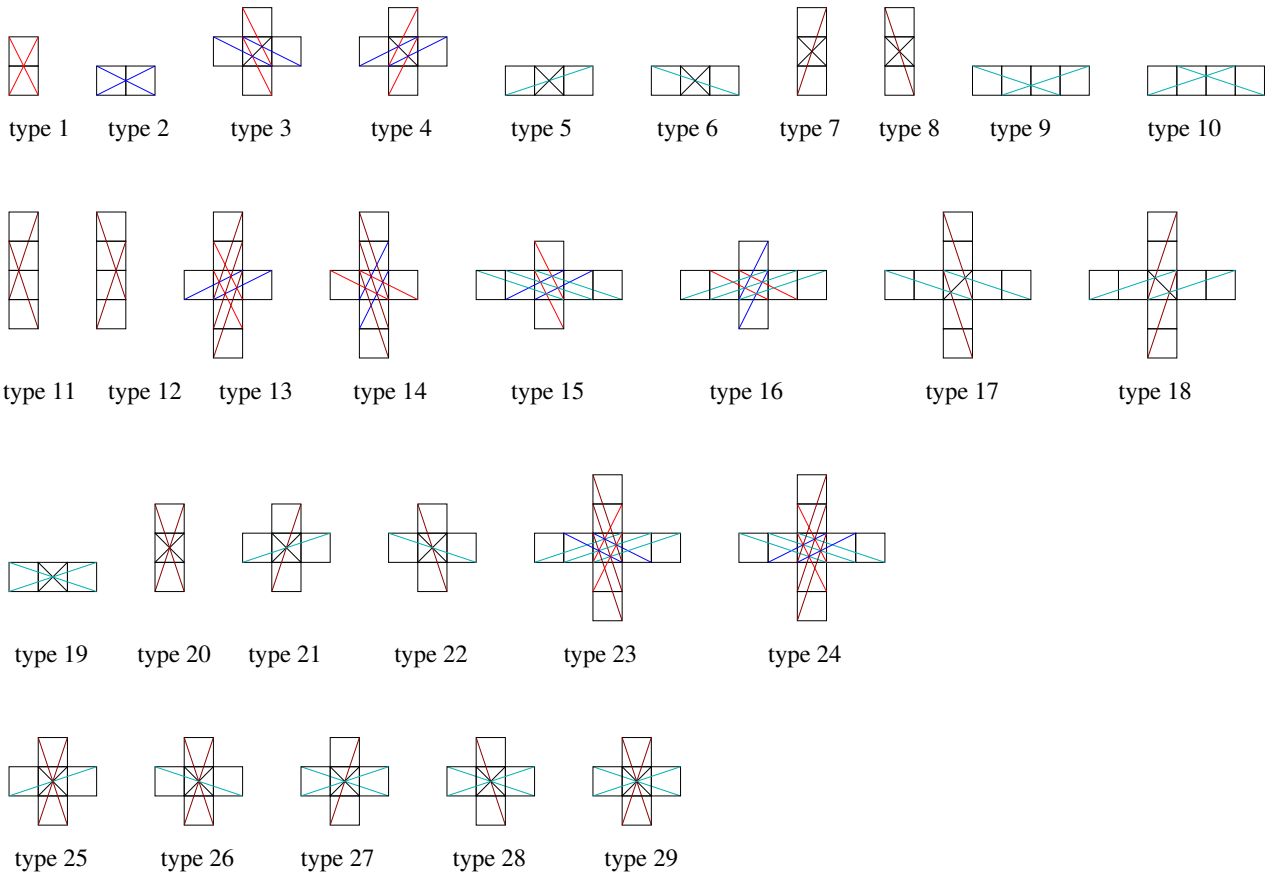

Figure 9: Types of incidences of 3, 4, 5, and 6 lines that are not at grid vertices: 3-wise crossings: types 1 through 18; 4-wise crossings: types 19 through 24; 5-wise crossings: types 25 through 28; 6-wise crossings: type 29.
For some types, the crossings are in the middle of a cell. To list the coordinates of crossing points, we rescale the grid cells to the unit square $[0,1]^2$.
For types 1 and 2, the crossings are at the midpoint of the horizontal and the vertical grid edges respectively. For type 3, the crossings are at $(1/3,1/3)$ and $(2/3,2/3)$.
For type 4, the crossings are at $(1/3,2/3)$ and $(2/3,1/3)$.
For types 9 and 10, the crossings are on vertical grid edges at height $1/3$ and $2/3$ from the horizontal line below, respectively.
For types 11 and 12, the crossings are on horizontal grid edges at distance $1/3$ and $2/3$ from the vertical line on the left, respectively.
For type 13, the crossings are at $(1/5,3/5)$ and $(3/5,4/5)$ and $(4/5,2/5)$ and $(2/5,1/5)$.
For type 14, the crossings are at $(1/5,2/5)$ and $(2/5,4/5)$ and $(4/5,3/5)$ and $(3/5,1/5)$.
For type 15, the crossings are at $(1/5,3/5)$ and $(3/5,4/5)$ and $(4/5,2/5)$ and $(2/5,1/5)$.
For type 16, the crossings are at $(1/5,2/5)$ and $(2/5,4/5)$ and $(4/5,3/5)$ and $(3/5,1/5)$.
For type 17, the crossings are at $(1/4,1/4)$ and $(3/4,3/4)$.
For type 18, the crossings are at $(1/4,3/4)$ and $(3/4,1/4)$.
For type 23, the crossings are at $(1/5,2/5)$ and $(2/5,4/5)$ and $(4/5,3/5)$ and $(3/5,1/5)$.
For type 24, the crossings are at $(1/5,3/5)$ and $(3/5,4/5)$ and $(4/5,2/5)$ and $(2/5,1/5)$.
For the other types, the crossings are at $(1/2,1/2)$.

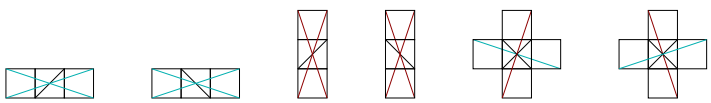

Figure 10: These incidence patterns cannot occur.

j	Bundles intersecting at type j vertices
1	$\mathcal{L}_2, \mathcal{L}_6, \mathcal{L}_{10}$
2	$\mathcal{L}_4, \mathcal{L}_8, \mathcal{L}_{12}$
3	$\mathcal{L}_2, \mathcal{L}_4, \mathcal{L}_9$
4	$\mathcal{L}_3, \mathcal{L}_8, \mathcal{L}_{10}$
5	$\mathcal{L}_3, \mathcal{L}_7, \mathcal{L}_9$
6	$\mathcal{L}_3, \mathcal{L}_5, \mathcal{L}_9$
7	$\mathcal{L}_3, \mathcal{L}_9, \mathcal{L}_{11}$
8	$\mathcal{L}_1, \mathcal{L}_3, \mathcal{L}_9$
9 & 10	$\mathcal{L}_5, \mathcal{L}_7, \mathcal{L}_{12}$

j	Bundles intersecting at type j vertices
11 & 12	$\mathcal{L}_1, \mathcal{L}_6, \mathcal{L}_{11}$
13	$\mathcal{L}_2, \mathcal{L}_8, \mathcal{L}_{11}$
14	$\mathcal{L}_1, \mathcal{L}_4, \mathcal{L}_{10}$
15	$\mathcal{L}_2, \mathcal{L}_5, \mathcal{L}_8$
16	$\mathcal{L}_4, \mathcal{L}_7, \mathcal{L}_{10}$
17	$\mathcal{L}_1, \mathcal{L}_5, \mathcal{L}_9$
18	$\mathcal{L}_3, \mathcal{L}_7, \mathcal{L}_{11}$
19	$\mathcal{L}_3, \mathcal{L}_5, \mathcal{L}_7, \mathcal{L}_9$
20	$\mathcal{L}_1, \mathcal{L}_3, \mathcal{L}_9, \mathcal{L}_{11}$

j	Bundles intersecting at type j vertices
21	$\mathcal{L}_3, \mathcal{L}_7, \mathcal{L}_9, \mathcal{L}_{11}$
22	$\mathcal{L}_1, \mathcal{L}_3, \mathcal{L}_5, \mathcal{L}_9$
23	$\mathcal{L}_1, \mathcal{L}_4, \mathcal{L}_7, \mathcal{L}_{10}$
24	$\mathcal{L}_2, \mathcal{L}_5, \mathcal{L}_8, \mathcal{L}_{11}$
25	$\mathcal{L}_1, \mathcal{L}_3, \mathcal{L}_7, \mathcal{L}_9, \mathcal{L}_{11}$
26	$\mathcal{L}_1, \mathcal{L}_3, \mathcal{L}_5, \mathcal{L}_9, \mathcal{L}_{11}$
27	$\mathcal{L}_3, \mathcal{L}_5, \mathcal{L}_7, \mathcal{L}_9, \mathcal{L}_{11}$
28	$\mathcal{L}_1, \mathcal{L}_3, \mathcal{L}_5, \mathcal{L}_7, \mathcal{L}_9$
29	$\mathcal{L}_1, \mathcal{L}_3, \mathcal{L}_5, \mathcal{L}_7, \mathcal{L}_9, \mathcal{L}_{11}$

Table 5: Bundles intersecting at type j vertices for $j = 1, 2, \ldots, 29$.

- For types $9, 10, 11, 12$, there is one crossing on the boundary of each grid cell; and

$$w_9 = \text{area}(\Gamma_5 \cap \Gamma_7 \cap \Gamma_{12}) = \text{area}(\Gamma_5 \cap \Gamma_7) = \text{area}(P(9, 10, 13, 14)) = \frac{1}{6}.$$

  Type 10 is the reflection in a horizontal line of type 9, and types 11 and 12 are 90° rotations of types 9 and 10, respectively. Therefore by symmetry, $w_9 = w_{10} = w_{11} = w_{12}$.

- For types $13, 14, 15, 16$, there are four crossings per grid cell; and

$$w_{13} = 4 \cdot (\text{area}(\Gamma_2 \cap \Gamma_8 \cap \Gamma_{11} \cap \overline{\Gamma_5})) = 4 \cdot (\text{area}(3, 9, 13) + \text{area}(4, 10, 16)) = \frac{1}{5}.$$

  Type 14 is the reflection in a vertical line of type 13, and types 15 and 16 are 90° rotations of types 13 and 14, respectively. Therefore by symmetry, $w_{13} = w_{14} = w_{15} = w_{16}$.

- For types 17 and 18, there are two crossings per grid cell; and

$$w_{17} = 2 \cdot (\text{area}(\Gamma_1 \cap \Gamma_5 \cap \Gamma_9)) = 2 \cdot (\text{area}(\Gamma_1 \cap \Gamma_5)) = 2 \cdot \text{area}(P(1, 2, 9, 10)) = \frac{1}{4}.$$

  Type 18 is the reflection in a vertical line of type 17; therefore by symmetry, $w_{17} = w_{18}$.

Consequently, we have

$$\lambda_3(m) = \frac{a_3 + \sum_{j=1}^{18} w_j}{\text{area}(\sigma_0)} - O(m) = \left(\frac{4}{3} + \frac{1}{2} + 1 + \frac{1}{10} + \frac{1}{10} + \frac{1}{3} + \frac{1}{3} + \frac{4}{5} + \frac{1}{2}\right) m^2 - O(m) = 5m^2 - O(m).$$

The values of $\lambda_i(m)$, for $i = 3, \ldots, 12$, are summarized in Table 7; for convenience the linear terms are omitted. Since $m = n/12$, λ_i can be also viewed as a function of n.

The multiplicative factor in Eq. (1.3) is bounded from below as follows:

$$\begin{aligned} F(n) \geq \prod_{i=3}^{12} B_i^{\lambda_i(n)} \geq\ & 2^{\frac{5n^2}{144}} \cdot 8^{\frac{103n^2}{60 \cdot 144}} \cdot 62^{\frac{2n^2}{5 \cdot 144}} \cdot 908^{\frac{13n^2}{60 \cdot 144}} \\ & \cdot 24698^{\frac{11n^2}{105 \cdot 144}} \cdot 1232944^{\frac{13n^2}{105 \cdot 144}} \cdot 112018190^{\frac{4n^2}{105 \cdot 144}} \\ & \cdot 18410581880^{\frac{n^2}{20 \cdot 144}} \cdot 5449192389984^{\frac{n^2}{30 \cdot 144}} \\ & \cdot 2894710651370536^{\frac{n^2}{12 \cdot 144}} \cdot 2^{-O(n)}. \end{aligned}$$

We prove by induction on n that $T(n) \geq 2^{cn^2 - O(n \log n)}$ for a suitable constant $c > 0$. It suffices to choose c (using the values of B_i for $i = 3, \ldots, 12$ in Table 1) so that

$$\begin{aligned} \frac{1}{144} \Bigg(& 5 + \frac{103}{60} \log 8 + \frac{2}{5} \log 62 + \frac{13}{60} \log 908 \\ & + \frac{11}{105} \log 24698 + \frac{13}{105} \log 1232944 \\ & + \frac{4}{105} \log 112018190 + \frac{1}{20} \log 18410581880 \\ & + \frac{1}{30} \log 5449192389984 \\ & + \frac{1}{12} \log 2894710651370536 \Bigg) \geq \frac{11c}{12}. \end{aligned}$$

The above inequality holds if we set

$$c = \frac{1}{132} \Bigg(5 + \frac{103}{60} \log 8 + \frac{2}{5} \log 62 + \frac{13}{60} \log 908 + \frac{11}{105} \log 24698 + \frac{13}{105} \log 1232944$$

j	w_j
1	1/4
2	1/4
3	1/2
4	1/2
5	1/20
6	1/20
7	1/20

j	w_j
8	1/20
9 & 10	1/3
11 & 12	1/3
13	1/5
14	1/5
15	1/5
16	1/5

j	w_j
17	1/4
18	1/4
19	1/15
20	1/15
21	1/40
22	1/40
23	2/5

j	w_j
24	2/5
25	1/120
26	1/120
27	1/120
28	1/120
29	1/12

Table 6: Values of w_j for $j = 1, \ldots, 29$.

i	3	4	5	6	7	8	9	10	11	12
$\lambda_i(m)$	$5m^2$	$\frac{103m^2}{60}$	$\frac{2m^2}{5}$	$\frac{13m^2}{60}$	$\frac{11m^2}{105}$	$\frac{13m^2}{105}$	$\frac{4m^2}{105}$	$\frac{m^2}{20}$	$\frac{m^2}{30}$	$\frac{m^2}{12}$
$\lambda_i(n)$	$\frac{5n^2}{144}$	$\frac{103n^2}{60\cdot144}$	$\frac{2n^2}{5\cdot144}$	$\frac{13n^2}{60\cdot144}$	$\frac{11n^2}{105\cdot144}$	$\frac{13n^2}{105\cdot144}$	$\frac{4n^2}{105\cdot144}$	$\frac{n^2}{20\cdot144}$	$\frac{n^2}{30\cdot144}$	$\frac{n^2}{12\cdot144}$

Table 7: The asymptotic values of $\lambda_i(m)$ and $\lambda_i(n)$ for $i = 3, \ldots, 12$.

$$+\frac{4}{105}\log 112018190 + \frac{1}{20}\log 18410581880$$
$$+\frac{1}{30}\log 5449192389984 + \frac{1}{12}\log 2894710651370536\Big)$$
$$> 0.2053,$$

and the lower bound in Theorem 1.1 follows.

4 Hexagonal construction with 6 slopes

Let H be a regular hexagon whose side has unit length. Consider 6 bundles of parallel lines whose slopes are $0, \infty, \pm 1/\sqrt{3}, \pm\sqrt{3}$. Three parallel strips are bounded by the pairs of lines supporting opposite sides of H, while the other three parallel strips are bounded by the pairs of lines supporting opposite short diagonals of H. The axes of all six parallel strips are incident to the center of the circle; see Fig. 11 (left). This construction[3] yields the lower bound $b_n \geq 0.1981n^2$ for large n.

Assume a coordinate system where the lower left corner of H is at the origin, and the lower side of H lies along the x-axis. Let $\mathcal{L} = \mathcal{L}_1 \cup \ldots \cup \mathcal{L}_6$ be the partition of $\mathcal{L}$ into six bundles of parallel lines. The m lines in $\mathcal{L}_i$ are contained in the parallel strip bounded by the two lines ℓ_{2i-1} and ℓ_{2i}, for $i = 1, \ldots, 6$. The equation of line ℓ_i is $\alpha_i x + \beta_i y + \gamma_i = 0$, with $\alpha_i, \beta_i, \gamma_i$, $i = 1, \ldots, 12$, given in Fig 11 (right).

We refer to lines in $\mathcal{L}_1 \cup \mathcal{L}_3 \cup \mathcal{L}_5$ as the *primary* lines, and to lines in $\mathcal{L}_2 \cup \mathcal{L}_4 \cup \mathcal{L}_6$ as *secondary* lines. Note that

- the distance between consecutive lines in any of the bundles of primary lines is $\frac{\sqrt{3}}{m}\left(1 - O\left(\frac{1}{m}\right)\right)$;
- the distance between consecutive lines in any of the bundles of secondary lines is $\frac{1}{m}\left(1 - O\left(\frac{1}{m}\right)\right)$.

Let $\sigma_0 = \sigma_0(m)$ and $\delta_0 = \delta_0(m)$ denote the basic parallelogram and triangle respectively, determined by the lines in $\mathcal{L}_1 \cup \mathcal{L}_3 \cup \mathcal{L}_5$; the side length of σ_0 and δ_0 is $\frac{2}{m}\left(1 - O\left(\frac{1}{m}\right)\right)$. Let H' be the smaller regular hexagon bounded by the short diagonals of H; the similarity ratio $\rho(H', H)$ is equal to $\frac{1}{\sqrt{3}}$. Recall that (i) the area of an equilateral triangle of side s is $\frac{s^2\sqrt{3}}{4}$; and (ii) the area of a regular hexagon of side s is $\frac{s^2 3\sqrt{3}}{2}$; as such, we have

$$\begin{aligned}
\text{area}(H) &= \frac{3\sqrt{3}}{2},\\
\text{area}(H') &= \frac{\text{area}(H)}{3} = \frac{\sqrt{3}}{2},\\
\text{area}(\delta_0) &= \frac{4}{m^2}\frac{\sqrt{3}}{4}\left(1 - O\left(\frac{1}{m}\right)\right)\\
&= \frac{\sqrt{3}}{m^2}\left(1 - O\left(\frac{1}{m}\right)\right),\\
\text{area}(\sigma_0) &= 2 \cdot \text{area}(\delta_0) = \frac{2\sqrt{3}}{m^2}\left(1 - O\left(\frac{1}{m}\right)\right).
\end{aligned}$$

For $i = 3, 4, 5, 6$, let a_i denote the area of the (not necessarily connected) region covered by exactly i of the 6 strips. The following observations are in order: (i) the six isosceles triangles based on the sides of H inside H have unit base and height $\frac{1}{2\sqrt{3}}$; (ii) the six smaller equilateral triangles incident to the vertices of

[3] If desired, this section can be skipped.

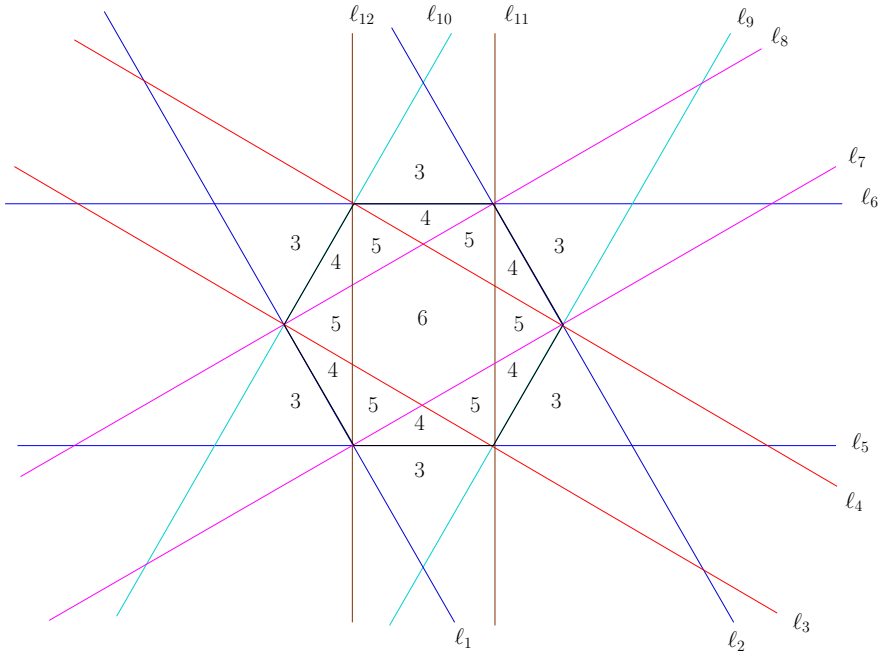

i	α_i	β_i	γ_i
1	$\sqrt{3}$	1	0
2	$\sqrt{3}$	1	$-2\sqrt{3}$
3	1	$\sqrt{3}$	-1
4	1	$\sqrt{3}$	-3
5	0	1	0
6	0	1	$-\sqrt{3}$
7	-1	$\sqrt{3}$	0
8	-1	$\sqrt{3}$	-2
9	$-\sqrt{3}$	1	$\sqrt{3}$
10	$-\sqrt{3}$	1	$-\sqrt{3}$
11	-1	0	1
12	-1	0	0

Figure 11: Left: The six parallel strips and corresponding covering multiplicities. These numbers only show incidences at the 3-wise crossings made by primary lines. Right: Coefficients of the lines ℓ_i for $i = 1, \ldots, 12$.

H have side-length $\frac{1}{\sqrt{3}}$. These observations yield

$$a_3 = \text{area}(H) = \frac{3\sqrt{3}}{2},$$
$$a_4 = 6 \cdot \text{area}(3,5,7) = 6 \cdot \frac{1}{4\sqrt{3}} = \frac{\sqrt{3}}{2},$$
$$a_5 = 6 \cdot \text{area}(3,7,11) = 6 \cdot \frac{1}{3}\frac{\sqrt{3}}{4} = \frac{\sqrt{3}}{2},$$
$$a_6 = \text{area}(H') = \frac{\sqrt{3}}{2}.$$

Observe that $a_4 + a_5 + a_6 = \text{area}(H)$. Recall that $\lambda_i(m)$ denote the number i-wise crossings where each bundle consists of m lines. Note that $\lambda_i(m)$ is proportional to a_i, for $i = 4, 5, 6$. Indeed, $\lambda_i(m)$ is equal to the number of 3-wise crossings of lines in $\mathcal{L}_1 \cup \mathcal{L}_3 \cup \mathcal{L}_5$ that lie in a region covered by i parallel strips, which is roughly equal to the ratio $\frac{a_i}{\text{area}(\sigma_0)}$, for $i = 4, 5, 6$. More precisely, taking also the boundary effect of the relevant regions into account, we obtain

$$\lambda_4(m) = \frac{a_4}{\text{area}(\sigma_0)} - O(m) = \frac{\sqrt{3}}{2}\frac{m^2}{2\sqrt{3}} - O(m)$$
$$= \frac{m^2}{4} - O(m),$$
$$\lambda_5(m) = \frac{a_5}{\text{area}(\sigma_0)} - O(m) = \frac{m^2}{4} - O(m),$$
$$\lambda_6(m) = \frac{a_6}{\text{area}(\sigma_0)} - O(m) = \frac{m^2}{4} - O(m).$$

For estimating $\lambda_3(m)$, the situation is little bit different, namely, in addition to considering 3-wise crossings of the primary lines, we also have 3-wise crossings of the secondary lines at the centers of the small equilateral triangles contained in H'. See Fig. 12. It follows that

$$\lambda_3(m) = \frac{a_3}{\text{area}(\sigma_0)} + \frac{\text{area}(H')}{\text{area}(\delta_0)} - O(m)$$
$$= \frac{3m^2}{4} + \frac{m^2}{2} - O(m) = \frac{5m^2}{4} - O(m).$$

The values of $\lambda_i(m)$, for $i = 3, 4, 5, 6$, are summarized in Table 8; for convenience the linear terms are omitted. Since $m = n/6$, λ_i can be also viewed as a function of n.

i	3	4	5	6
$\lambda_i(m)$	$\frac{5m^2}{4}$	$\frac{m^2}{4}$	$\frac{m^2}{4}$	$\frac{m^2}{4}$
$\lambda_i(n)$	$\frac{5n^2}{4\cdot 36}$	$\frac{n^2}{4\cdot 36}$	$\frac{n^2}{4\cdot 36}$	$\frac{n^2}{4\cdot 36}$

Table 8: The asymptotic values of $\lambda_i(m)$ and $\lambda_i(n)$ for $i = 3, 4, 5, 6$.

The multiplicative factor in Eq. (1.3) is bounded

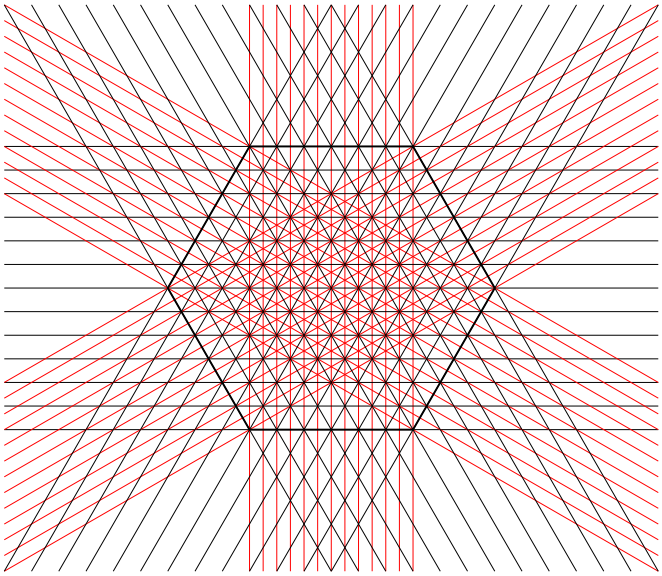

Figure 12: Triple incidences of secondary lines (drawn in red).

from below as follows:

$$F(n) \geq \prod_{i=3}^{6} B_i^{\lambda_i(n)} \geq 2^{5n^2/144} \cdot 8^{n^2/144} \cdot 62^{n^2/144} \cdot 908^{n^2/144} \cdot 2^{-O(n)}.$$

We prove by induction on n that $T(n) \geq 2^{cn^2 - O(n \log n)}$ for a suitable constant $c > 0$. It suffices to choose c (using the values of B_i for $i = 3, 4, 5, 6$ in Table 1) so that

$$\frac{8 + \log 62 + \log 908}{144} \geq \frac{5c}{6}.$$

The latter inequality holds if we set

$$c = \frac{\log(256 \cdot 62 \cdot 908)}{120} > 0.1981,$$

and the lower bound follows.

5 Conclusion

We analyzed several recursive constructions derived from arrangements of lines with 3, 4, 6, 8, and 12 distinct slopes in a rectangular style and 6 distinct slopes in a hexagonal style. Among these, the best lower bound is $b_n \geq 0.2053n^2$ for large n; as offered by the rectangular construction with 12 slopes.

Subsequent to submission of our paper, we developed and analyzed a hexagonal construction with 12 distinct slopes that yields a lower bound of $b_n \geq 0.2083\, n^2$ for large n; see [3]. We have little doubt that increasing the number of slopes will further increase the lower bound, and the proof complexity at the same time. The question of how far can one go is likely to remain out there. We conclude with the following questions.

1. What lower bounds on B_n can be deduced from line arrangements with a higher number of slopes? In particular, hexagonal and rectangular constructions with 16 slopes seem to be the most promising candidates. Note that the value of B_{16} is currently unknown.
2. What lower bounds on B_n can be obtained from rhombic tilings of a centrally symmetric octagon? Or from those of a centrally symmetric k-gon for some other even $k \geq 10$? No closed formulas for the number of such tilings seem to be available at the time of the present writing. However, suitable estimates could perhaps be deduced from previous results; see, e.g., [1, 2, 4, 12].

Acknowledgment. The authors thank two anonymous reviewers who spotted a small calculation error in a previous version (in Eq. (2.5) at the end of Section 2).

References

[1] N. Destainville, R. Mosseri, and F. Bailly, Fixed-boundary octagonal random tilings: a combinatorial approach, *Journal of Statistical Physics* **102(1-2)** (2001), 147–190.
[2] N. Destainville, R. Mosseri, and F. Bailly, A formula for the number of tilings of an octagon by rhombi, *Theoretical Computer Science* **319** (2004), 71–81.
[3] A. Dumitrescu and R. Mandal, New lower bounds for the number of pseudoline arrangements, preprint available at `https://arxiv.org/abs/1809.03619`.
[4] S. Elnitsky, Rhombic tilings of polygons and classes of reduced words in Coxeter groups, *Journal of Combinatorial Theory Ser. A* **77** (1997), 193–221.
[5] V. Elser, Solution of the dimer problem on an hexagonal lattice with boundary, *Journal of Physics A: Mathematical and General* **17:**1509 (1984).
[6] S. Felsner, On the number of arrangements of pseudolines, *Discrete & Computational Geometry* **18** (1997), 257–267.
[7] S. Felsner, *Geometric Graphs and Arrangements*, Advanced Lectures in Mathematics, Vieweg Verlag, 2004.
[8] S. Felsner and J. E. Goodman, Pseudoline arrangements, in *Handbook of Discrete and Computational Geometry* (3rd edition), (J. E. Goodman, J. O'Rourke, C. D. Tóth, editors), CRC Press, Boca Raton (2017), pp. 125–157.
[9] S. Felsner and P. Valtr, Coding and counting arrangements of pseudolines, *Discrete & Computational Geometry* **46(4)** (2011), 405–416.

[10] J. E. Goodman and R. Pollack, A combinatorial perspective on some problems in geometry, *Congressus Numerantium* **32** (1981), 383–394.

[11] J. E. Goodman and R. Pollack, Allowable sequences and order types in discrete and computational geometry, in *New Trends in Discrete and Computational Geometry* (J. Pach, editor), Algorithms and Combinatorics, Volume 10, Springer, New York, 1993, pp. 103–134.

[12] M. Hutchinson and M. Widom, Enumeration of octagonal tilings, *Theoretical Computer Science* **598** (2015), 40–50.

[13] J. Kawahara, T. Saitoh, R. Yoshinaka, and S. Minato. Counting primitive sorting networks by πDDs. Technical Report, Hokkaido University, TCS-TR-A-11-54, 2011. `http://www-alg.ist.hokudai.ac.jp/~thomas/TCSTR/tcstr_11_54/tcstr_11_54.pdf`

[14] D. E. Knuth, *Axioms and Hulls*, Lecture Notes in Computer Science, Vol. 606, Springer, Berlin, 1992.

[15] D. E. Knuth, *The Art of Computer Programming, Vol. 3: Sorting and Searching*, 2nd edition, Addison–Wesley, Reading, MA, 1998.

[16] Jan Kynčl, Improved enumeration of simple topological graphs, *Discrete & Computational Geometry* **50(3)** (2013), 727–770.

[17] P. A. MacMahon, *Combinatory Analysis*, vol. II, Chelsea, New York, 1960. Reprint of the 1916 edition.

[18] J. Matoušek, *Lectures on Discrete Geometry*, Springer, New York, 2002.

[19] N. Sloane and S. Plouffe, The On-Line Encyclopedia of Integer Sequences, `http://oeis.org/A006245` (accessed March 11, 2018).

[20] R. Stanley, On the number of reduced decompositions of elements of Coxeter groups, *European Journal of Combinatorics* **5** (1984), 359–372.

[21] K. Yamanaka, S. Nakano, Y. Matsui, R. Uehara, and K. Nakada, Efficient enumeration of all ladder lotteries and its application, *Theoretical Computer Science* **411(16-18)** (2010), 1714–1722.